ap

Asian Journal of Physics

Vol. 28, Nos 7-9 (2019) 487-498

Available on: www.asianjournalofphysics.in

Light propagation through graded-index fibers: Impact of self-imaging on the nonlinear phenomena

Govind P Agrawal

The Institute of Optics, University of Rochester, Rochester, NY, 14627, USA

Invited paper dedicated to Professor Ajoy Ghatak on his 80th Birthday

Periodic self-imaging of optical beams inside graded-Index (GRIN) fibers has been known for more than 45 years. It has been found in recent years that spatial self-imaging also affects the nonlinear temporal evolution of optical pulses inside such fibers. In a 1974 paper that I coauthored with Prof Ghatak [1], it was shown that, in the absence of the nonlinear effects, the optical field at any point inside the GRIN fiber can be written in an analytic form without any explicit reference to its modes. The result was in the form of a propagation kernel that reproduced the input field precisely in a periodic fashion along the length of the GRIN fiber (self-imaging property).We apply this kernel first to a Gaussian beam and discuss how self-imaging affects the nonlinear effects such as modulation instability and supercontinuum generation. We then consider the impact of the spatial shape and position of the input beam (at the input facet of the fiber) on the nonlinear effects by considering off-center launch of a Gaussian beam and a circular beam with uniform intensity. The results show that the results obtained in our 1974 paper are still useful for studying nonlinear optical phenomena in modern GRIN fibers

Keywords: Graded-index fibers, Self-imaging, Nonlinear optics, Modulation instability, Supercontinuum generation

1 Introduction

I was a graduate student from 1969 to 1974 at the Indian Institute of Technology Delhi (IITD), where I had the pleasure of having Prof Ajoy Ghatak first as a teacher and then as a mentor. Even though he was not my thesis adviser, I coauthored a paper with him that was published in November 1974 (close to his 35th birthday). This paper studied propagation of partially coherent light through a graded-index (GRIN) fiber [1]. Such fibers were studied during the 1970s, motivated mostly by their applications in optical communication systems [2-5]. The interest in GRIN fibers declined during the 1980s as the use of single-mode fibers became dominant for such systems. It was only after 2010 that multimode fibers attracted renewed attention for enhancing the capacity of optical communication systems through space-division multiplexing [6-8]. This revival led to a resurgence of interest in GRIN fibers, especially in their nonlinear properties [9-14]. Among the nonlinear phenomena that have attracted attention are soliton formation inside GRIN fibers [10, 15], geometric parametric instability [11], and spatial-beam cleanup [12]. Our 1974 paper has not been referenced in the recent literature. I discovered in 2018 that this paper is quite relevant for nonlinear propagation in GRIN fibers and have pointed this out in my recent review on GRIN fibers [16]. At the occasion of the 80th birthday on Nov 9, 2019 of Prof Ghatak, I discuss here how our collaboration is making an impact even after 45 years.

The paper is organized as follows. In Section 2, I discuss theory behind self-imaging using a modal-expansion approach and show that the output field at any point inside the fiber can be obtained, without any

Corresponding author :

e-mail: govind.agrawal@rochester.edu (Govind P Agrawal)

reference to the fiber modes, using a result first obtained in our 1974 paper. I apply this kernel in Section 3 to study the propagation of a Gaussian beam inside a GRIN fiber and recover a known result for its periodically varying beam width. The nonlinear effects are discussed in Section 4, where I present an effective nonlinear Schrödinger equation that includes the effects of periodic self-imaging. I show in Section 5 how the self-imaging theory of Section 2 can be sued to study the impact of input beam's position and shape on the nonlinear phenomenon such as modulation instability. Finally, the main results are summarized in Section 5.

2 Self-imaging in GRIN fibers

The modes of GRIN fibers are obtained by solving the Helmholtz equation

$$\nabla^2 \mathbf{E} + n^2(x, y)\, k_0^2 \mathbf{E} = 0. \tag{1}$$

where $k_0 = \omega/c$ at the optical frequency ω. The refractive index of most GRIN fibers decreases radially inside the core of radius a from its value n_1 at the center to the cladding index n_c as [17]

$$n^2(x, y) = n_1^2\, [1 - 2\Delta\, (x^2 + y^2)/a^2], \tag{2}$$

where the parameter $\Delta = (n_1 - n_c)/n_1$ plays an important role and is defined in the same way as for step-index fibers [18]. Although a numerical approach is necessary in general, Eq (1) can be solved analytically if we assume that the index profile in Eq (2) applies for all values of x and y. Assuming that the electric field varies as $\mathbf{E}(x, y, z) = \hat{\mathbf{x}} F(x, y) e^{i\beta z}$, the fiber modes are obtained by solving

$$\frac{\partial^2 F}{\partial x^2} + \frac{\partial^2 F}{\partial y^2} + [n^2(x, y)\, k_0^2 - \beta^2] F = 0. \tag{3}$$

where β is the propagation constant. The GRIN problem is closely related to finding the quantized energy states of a two-dimensional harmonic oscillator. In both cases, the solution for $F(x, y)$ are related to the Hermite–Gaussian functions.

In the case of a GRIN fiber, the modes are denoted as LP_{mn}, where m and n are two integers used for labeling different modes. Their modal distribution $F_{mn}(x, y)$ and propagation constants β_{mn} are known. We refer to Ref. [17] for the expressions of mode profiles $F_{mn}(x, y)$ and write here the modal propagation constants given by

$$\beta_{mn} = n_1 k_0 \left[1 - \frac{2(m+n-1)}{n_1 k_0 a}\sqrt{2\Delta}\right]^{1/2}. \tag{4}$$

For most GRIN fibers, $k_0 a \le 1$ and $\Delta \le 0.01$. As a result, as long as $m + n$ is not too large, we can expand β_{mn} in a binomial series and approximate it as

$$\beta_{mn} \approx n_1 k_0 - (m + n - 1)\sqrt{2\Delta}/a. \tag{5}$$

This equation reveals the most important feature of the modes of a GRIN fiber. It shows that the propagation constants modes form a ladder-like structure with equal spacing between any two neighboring modes. This feature is analogous to the energy levels of a harmonic oscillator and is the physical mechanism behind the self-imaging phenomenon in GRIN fibers.

An optical beam with the input field $E(x, y, 0)$, in general, excites multiple fiber modes such that

$$E(x, y, 0) = \sum_m \sum_n c_{mn} F_{mn}(x, y), \tag{6}$$

where the sum extends over the whole range of the two integers ($m, n = 0$ to ∞) and we assume that all modes have been normalized such that

$$\iint_{-\infty}^{\infty} F_{mn}(x, y)\, F^*_{m'n'}(x, y)\, dx\, dy = \delta_{mm'} \delta_{nn'}. \tag{7}$$

The expansion coefficients c_{mn} are found by multiplying Eq (6) with $F^*_{m'n'}(x, y)$ and integrating over the whole transverse plane. The result is given by

$$c_{mn} = \iint_{-\infty}^{\infty} F^*_{m'n'}(x, y)\, E(x, y, 0)\, dx\, dy \tag{8}$$

The optical field $E(x, y, z)$ at any point inside the GRIN fiber is obtained by multiplying each mode with a phase factor such that

$$E(x, y, 0) = \sum_m \sum_n c_{mn} F_{mn}(x, y) \exp(i\beta_{mn} z). \tag{9}$$

Substituting c_{mn} from Eq (8), we can write the result in the form

$$E(x, y, 0) = \iint_{-\infty}^{\infty} K(x, x'\,; y, y')\, E\,(x, y', 0)\, dx'\, dy' \tag{10}$$

where the propagation kernel is given by

$$K(x, x'; y, y') = \sum_m \sum_n F_{mn}(x, y)\, F^*_{mn}(x', y')\, \mathrm{e}^{i\beta_{mn} z}. \tag{11}$$

The form of Eq (10) is similar to that used for diffraction of optical beams inside a homogeneous medium of constant refractive index. If the double sum in Eq (11) can be evaluated in a closed form, the resulting kernel will include all of the excited modes of a GRIN fiber, without any explicit reference to them. It was shown [1] in 1974 that the double sum can be carried out analytically for GRIN fibers because of the ladder-like structure of the modal propagation constants [1]. The final result is given by

$$K(x, x'; y, y') = \frac{\beta}{2\pi i}\left(\frac{b e^{i\psi}}{\sin(bz)}\right) \exp\left(\frac{i\beta b}{2\sin(bz)}[\cos(bz)(x'^2 + y'^2) - 2(xx' + yy')]\right) \tag{12}$$

where $\beta = n_1 k_0$, $b = \sqrt{2\Delta}/a$, and the phase ψ depends only on the location of the point $\mathbf{r} = (x, y, z)$ as

$$\psi(\mathbf{r}) = \beta z + \frac{1}{2}\beta b \cot(bz)(x^2 + y^2). \tag{13}$$

Noting that $\sin(bz)/b = z$ in the limit $b \to 0$, it is easy to see that the kernel in Eq (14) reduces to

$$K(x, x'; y, y') = \frac{b e^{i\beta z}}{2\pi i z} \exp\left(\frac{i\beta}{2z}[(x - x')^2 + (y - y')^2]\right) \tag{14}$$

which is the form expected for a homogeneous medium of constant refractive index.

It is well known that a GRIN fiber reproduces its input field periodically along its length. This self-imaging property follows from the observation that the kernel in Eq (12) is reduced to the form

$$K(x, x'; y, y') = \delta(x - x')\, \delta(y - y')\mathrm{e}^{i\beta z} \tag{15}$$

at distances that are integer multiples of the fundamental period $2\pi/b$. This can be seen by noting that $\cos(bz)$ can be replaced with 1 at such distances and K in Eq (12) can be written as $K = f\,(x - x')\, f\,(y - y')\mathrm{e}^{ikz}$, where the function $f\,(x)$ is defined as

$$f\,(x) = \sqrt{\frac{p}{\pi}}\, \mathrm{e}^{-px^2}, \qquad p = \frac{\beta b}{2i\sin(bz)}. \tag{16}$$

It is easy to see that $\int_{-\infty}^{\infty} f\,(x)\, dx = 1$. At distances $z = 2m\pi/b$, where m is an integer, p becomes infinitely large, and $f\,(x)$ is reduced to the delta function $\delta(x)$. It follows from Eqs (10) and (15) that the field $E(\mathbf{r})$ becomes identical to the input field at all such distances, resulting in self-imaging.

Self-imaging also occurs at a shorter distance $z_p = \pi/b$ with one major difference. In this case, the delta functions in Eq (15) are replaced with $\delta\,(x + x')$ and $\delta\,(y + y')$. As a result, $E(x, y, z_p) = E(\,x, y, 0)$, i.e., the image is flipped in both transverse directions. If the input field is radially symmetric, the sign changes have no impact, and the input field is reproduced (self-imaging) for the first time at the distance z_p and then periodically at distances that are multiples of z_p. It is important to stress that self-imaging at the distance $2z_p$ occurs for any arbitrary input field, without any restriction on its functional form. This is the reason why GRIN rods can be used as a lens. We refer to a 1976 paper for further details on the imaging characteristics of a GRIN medium [3]. In particular, it can be shown that the ratio $f = \cot(bz)/b$ plays the role of the focal length of such GRIN lenses. Self-imaging can occur even when the input beam is only partially coherent [19].

3 Self-imaging of a CW Gaussian beam

A Gaussian-shape input beam is often launched into a GRIN fiber. It is thus useful to apply Eq (10) to an input beam for which

$$E(x, y, 0) = A_0 \exp\left(-\frac{x^2+y^2}{2w_0^2}\right), \tag{17}$$

where A_0 is the peak amplitude and w_0 is the spot size(1/ewidth)of the Gaussian beam. We can find the electric field at any point $\mathbf{r} = (x, y, z)$ inside the fiber by using Eq (17) in Eq (10) together with the kernel in Eq (14).The two integrations can be performed by using the known integral

$$\int_{-\infty}^{\infty} \exp(-px^2 + qx)dx = \sqrt{\pi/p}\ \exp(q^2/4p). \tag{18}$$

The final result can be written as

$$E(\mathbf{r}) = A_0 F(\mathbf{r}) \exp[i\varphi(\mathbf{r})], \tag{19}$$

where the beam shape is governed by

$$F(\mathbf{r}) = \frac{w_0}{w(z)} \exp\left[-\frac{(x^2+y^2)}{2w^2(z)}\right], \tag{20}$$

and the phase $\phi(\mathbf{r})$ is given by

$$\phi(\mathbf{r}) = \frac{\beta}{2w}\frac{dw}{dz}(x^2+y^2) + \beta z + \tan^{-1}(C\tan bz). \tag{21}$$

Clearly, the shape of the beam remains Gaussian but its spatial width evolves with z in a periodic fashion as

$$w(z) = w_0\sqrt{\cos^2(\pi z/zp) + C^2\sin^2(\pi z/zp)}\ . \tag{22}$$

Here, the spatial period z_p and parameter C are defined as

$$z_p = \frac{\pi a}{\sqrt{2\Delta}}, \qquad C = \frac{z_p/\beta}{\pi w_0^2}, \tag{23}$$

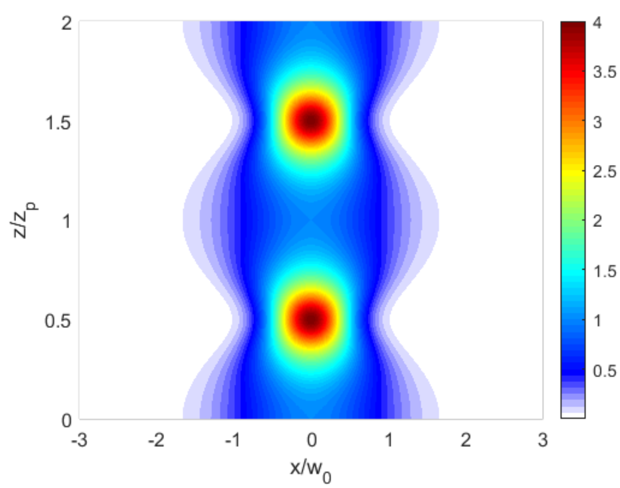

Fig 1. Evolution of a Gaussian beam inside a GRIN fiber over two self-imaging periods for $C = 0.5$. Cross-section along the $y = 0$ plane is shown with a color-coded intensity distribution.

These results show that the amplitude and width (also phase) of a Gaussian beam change in a periodic fashion such that the beam recovers all of its input features periodically at distances $z = mz_p$ (m is any positive integer) because of the self-imaging phenomenon. At distances $z = (m + 1/2)z_p$, the beam's width takes its minimum value w_0C, i.e., C governs the extent of beam compression during each cycle. As an example, Figure 1 shows the evolution of a Gaussian beam over two periods along the fiber's length using $C = 0.5$. For this value of C, the beam width is reduced by a factor of two at the point of maximum compression and its peak intensity is enhanced by a factor of 4. Compression by a factor of 10 and intensity enhancement by a factor of 100 can be realized by making $C = 0.1$.

Let us estimate the values of two parameters defined in Eq (23) for typical GRIN fibers. Using $\Delta = 0.01$ and $a = 25$ µm (typical values for commercial GRIN fibers), we find $z_p = 0.55$ mm, a remarkably short distance at which self-imaging first occurs inside such a GRIN fiber. Assuming $w_0 = 8$ µm and using $\beta = 2\pi n_1/\lambda$ with $n_1 = 1.45$ and $\lambda = 1.06$ µm, we find $C \approx 0.3$, indicating that the beam width is reduced to 30% of its initial value at $z_p/2$, before it recovers its input value at a distance of z_p. Even smaller values of C can be realized in practice by increasing the initial spot size w_0 of the Gaussian beam. Figure 2 shows how the ratio w/w_0 varies over one self-imaging period for several values of the parameter C.

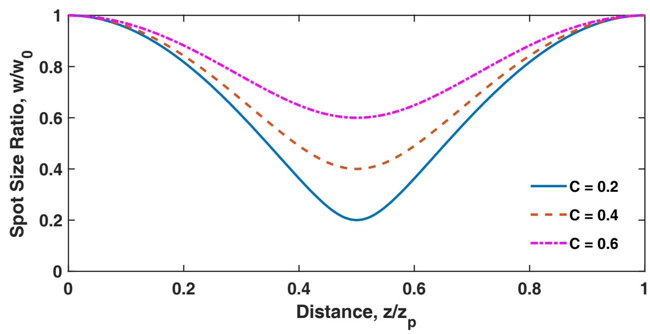

Fig 2. Beam-width ratio w/w_0 plotted over one self-imaging period for several values of the C parameter.

We should ask:what happens to the self-imaging property of GRIN fibers when input power becomes large enough that the Kerr nonlinearity of the silica material cannot be ignored ? It is known that the Kerr contribution to the refractive index can lead to self-focusing of an optical beam with intensity I even inside a homogeneous medium of constant refractive index. As a GRIN medium also reduces the beam size, the two effects may act together in such a way that catastrophic self-focusing occurs even at a shorter distance. Clearly, self-focusing can destroy the self-imaging property when input power is close to P_{cr}. The important question is whether self-imaging can occur when input power is well below P_{cr} , but the nonlinear effects cannot be ignored. This question was answered in 1992 by solving the Gaussian-beam propagation problem with the variational technique [21], after adding the nonlinear contribution n_2I to the refractive index $n(x, y)$ in Eq (2). It was found that the beam width oscillates as indicated in Eq (22) with the same period z_p but the parameter C in Eq (23) is modified as

$$C = \sqrt{1-(P/P_{cr})}\left(\frac{z_p/\beta}{\pi w_0^2}\right), \tag{24}$$

Even though the Kerr nonlinearity reduces the value of C parameter, it does not affect the period of self-imaging. In physical terms, the Kerr nonlinearity only enhances the extent of beam compression during each self-imaging cycle. As long as the input power of a CW beam remains below the critical level of self-focusing, periodic self-imaging occurs just as it would in the absence of the nonlinear effects.

4 Nonlinear Pulse Propagation

We consider next the propagation of a pulsed Gaussian beam inside a nonlinear GRIN fiber. The full problem is quite complicated because of its four-dimensional nature involving *x, y, z*, and *t*. A modal approach, often used in practice [22], requires solving many coupled equations with a large number of nonlinear terms and is limited in practice to fibers supporting a relatively small number of modes. It was found in 2017 that a simpler approach is possible for multimode GRIN fibers [13]. Its main assumption is that the bandwidth of the pulse is narrow enough that the spatial profile $F(\mathbf{r})$ of the beam does not vary much over this bandwidth. It is important to keep in mind that $F(\mathbf{r})$ is not the spatial profile of a specific mode but results from a superposition of all the modes excited by the input beam. After eliminating the transverse coordinates through a spatial integration and going back to the time domain, the amplitude $A(z, t)$ is found to satisfy [13]

$$\frac{\partial A}{\partial z} + \frac{i\beta_2}{2}\frac{\partial^2 A}{\partial T^2} = i\,\bar{\gamma}(z)|A|^2 A \tag{25}$$

where $T = t - z/v_g$, v_g is the group velocity, and β_2 governs group-velocity dispersion (GVD) of the fiber. The nonlinear parameter is defined as

$$\bar{\gamma}(z) = \frac{\omega_0 n_2}{cA_{eff}(z)}, \quad A_{eff}(z) = \left(\iint |F(\mathbf{r})|^4 dxdy\right)^{-1}. \tag{26}$$

We call $A_{eff}(z)$ the *effective beam area* to distinguish it from the *effective mode area*, whose value remains constant with z in single-mode fibers [18]. Equation (25) with a constant value of γ is known as the nonlinear Schrödinger (NLS) equation.

Equation (25) is remarkable. It shows that temporal evolution inside a GRIN fiber can be studied by solving a single NLS equation, even though multiple spatial modes may be propagating simultaneously inside the fiber. The oscillating spatial width resulting from the self-imaging property produces a nonlinear parameter $\bar{\gamma}(z)$ that is periodic in z. One can also interpret the same effect as a periodically varying effective beam area. The spatial integrals in Eq (26) can be performed analytically using the functional form of $F(\mathbf{r})$ in Eq (20) to obtain $\bar{\gamma}(z) = \gamma/f(z)$, where γ is defined using the initial value of A_{eff} at $z = 0$. Thus, Eq (25) becomes

$$\frac{\partial A}{\partial z} + \frac{i\beta_2}{2}\frac{\partial^2 A}{\partial T^2} = i\,\gamma f^{-1}(z)|A|^2 A \tag{27}$$

where the function $f(z)$ is found from Eq (22) and has the form

$$f(z) = 1 - (1 - C^2)\sin^2(\pi z/z_p). \tag{28}$$

It is easy to see that $f(z)$ represents the factor by which the effective are $A_{\text{eff}}(z)$ of the beam is reduced because of periodic self-imaging inside a GRIN fiber.

As a simple application, we can use Eq (27) to study the phenomenon of modulation instability. In the context of single-mode optical fibers [18], it occurs only in the anomalous-GVD region and converts a CW beam into a train of optical solitons. The stability of a CW Gaussian beam inside a GRIN fiber was studied [23] in 2003 using the analytic solution given in Eq (19). A more general analysis was carried out in 2019 in terms of a Hill's equation [24]. In both cases, the analysis is quite complicated. The modified NLS equation (27) provides a simpler approach for studying modulation instability in GRIN fibers [13]. The results show that a CW Gaussian beam can become unstable even when it propagates in the normal-GVD region of the fiber. The gain spectrum of modulation instability exhibits a rich structure with an infinite number of sideband pairs at frequencies that are not equally spaced. The peak gain of each sideband depends on the spatial pattern of the oscillating Gaussian beam through $f(z)$. Since spatial variations play a crucial role, this instability is also known as a geometric parametric instability [11]. The frequency shift of the mth sideband from the CW-beam frequency is given by [25]

$$\Omega_m = \pm\sqrt{\frac{2\pi m}{\beta_2 z_p} - \frac{2}{\beta_2 L_{NL} C}} \tag{29}$$

where m is an integer and $L_{\text{NL}} = (\gamma P_0)^{-1}$ is the nonlinear length. The $m = 0$ sideband exists only if $\beta_2 < 0$ at the pump wavelength. The sideband frequencies predicted by Eq (29) were seen in a 2016 experiment in which relatively long (900 ps) pulses at 1064 nm were launched into a 6-m-long GRIN fiber to mimic a quasi-CW situation [11].

The formation of solitons inside multimode fibers attracted attention during the 1980s [26, 27]. Theoretical work carried out during the 1990s indicated that the formation of temporal solitons was indeed feasible inside a GRIN medium [28-30]. It eventually led in 2013 to the observation of a multimode soliton [10]. In this experiment, the spatial width of the beam was so small that only three lowest-order modes of the fiber were excited. We used Eq (27) in 2018 to show that GRIN fibers support propagation of pulsed Gaussian beams that preserve their temporal shape and behave like a soliton, even though their spatial width oscillates along the fiber length [15]. We referred to such pulses as GRIN solitons to emphasize that a parabolic index profile is essential for their existence.

Equation (27) can also be used to study the fission of higher-order solitons that leads to the emission of multiple dispersive waves and broaden the pulse spectrum drastically to form a supercontinuum [18]. An important question is how this process is affected by the spatial oscillations of a pulsed Gaussian beam related to self-imaging. For this purpose, we modify Eq (27) to include the effects of third-order dispersion (TOD) and intrapulse Raman scattering:

$$i\frac{\partial U}{\partial \xi} + \frac{1}{2}\frac{\partial^2 U}{\partial \tau^2} - i\delta_3 \frac{\partial^3 U}{\partial \tau^3} + \frac{N^2}{f(\xi)} U(\xi,\tau) \int_0^\infty R(s)|U(\xi,\tau-s)|^2 ds = 0 \tag{30}$$

where δ_3 is the normalized TOD parameter and the nonlinear response function $R(t) = (1 - f_R)\delta(t) + f_R h_R(t)$ includes both the Kerr and Raman contributions with $f_R = 0.18$. An equation with a periodic nonlinear term similar to Eq (30) was first solved in Ref [32]; it was found to produce multiple dispersive waves at different frequencies that agreed well with the experimental results.

Figure 3 shows the temporal and spectral evolution of a third-order soliton ($N = 3$) inside a GRIN fiber over one dispersion length using $\delta_3 = 0.02$. The input pulse is taken to be 100-fs wide (FWHM). We used $C = 0.5$ for which the beam width is reduced by a factor of two during each self-imaging period. As expected, soliton fission occurs and a dispersive wave is produced at a blue-shifted frequency near $(\nu - \nu_0)T_0 = 5.5$. However, multiple additional dispersive waves are generated at both the red and the blue sides of the original spectrum. Also, intrapulse Raman scattering leads to a red-shift of the shortest soliton that is much larger in the case of a GRIN fiber compared to single-mode step-index fiber [33].

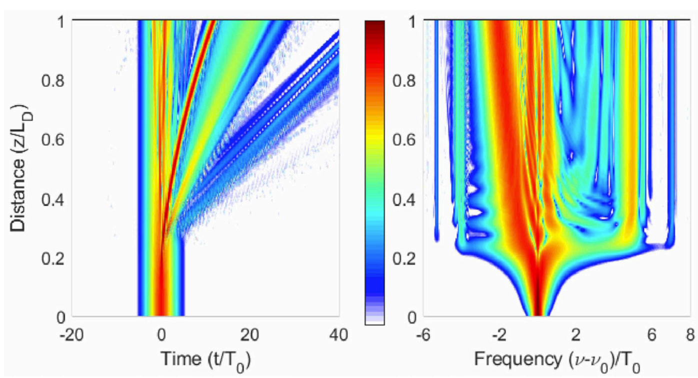

Fig 3. Temporal and spectral evolution of a third-order soliton ($N = 3$) inside a GRIN fiber over one dispersion length using $\delta_3 = 0.02$, $q = 100$ and $C = 0.5$.

The periodic self-imaging of the Gaussian beam affects the temporal evolution in Fig 3 in two ways. First, the effective value of the soliton order N is enhanced to 4.24 compared to its initial value of $N = 3$. As a result, the evolution in Fig 3 is closer to that occurring for a fourth-order soliton. This is the reason why the Raman-induced frequency shift is enhanced. Second, periodic self-imaging creates a nonlinear index grating through the Kerr effect because the refractive index is larger in the regions where the beam width is reduced and the intensity is enhanced locally. This grating creates the multiple dispersive waves seen in Fig 3. The frequencies of all dispersive waves can be calculated using the phase-matching condition ,and the numerical results agree with the predicted values.

5 Impact of input beam's position and shape

The propagation kernel that was found in my 1974 paper (coauthored with Prof. Ghatak) allows one to consider the impact of input beam's position and shape on the nonlinear effects inside GRIN fibers. As a simple example, consider first a Gaussian beam whose intensity peak does not coincide with the core center of the GRIN fiber. If its peak is shifted by a distance s along the x axis, the input field in Eq (17) is replaced with

$$E(x, y, 0) = A_0 \exp\left(-[(x-s)^2 + y^2]/2w_0^2\right). \tag{31}$$

The optical field at any point $\mathbf{r} = (x, y, z)$ inside the fiber is found using Eq (31) in Eq (10) together with the kernel in Eq (14). All integrals can be performed using the result in Eq (18).The final result can be written as in Eq (19), but the beam evolution is now governed by

$$F(\mathbf{r}) = \frac{w_0}{w(z)} \exp\left(\frac{[x - s\cos(bz)]^2 + y^2}{2w^2(z)}\right) \tag{32}$$

where $w(z)$ varies with z in a periodic fashion as given in Eq (22) with the parameters z_p and C as defined in Eq (23). Figure 4 shows how the Gaussian beam evolves along the fiber length by plotting $|F(x,0,z)|^2$ in the xz plane with the intensity color-coded on alogarithmic scale. Similar to the on-axis launch, the beam's width still oscillates with z, compressing and recovering its input value periodically. The new feature is that the beam's center also oscillates in a periodic fashion around $x = 0$. As a result, even though the Gaussian beam recovers its initial width w_0 at the distance $z = z_p$, its self-imaging does not occur at that point because the beam is centered at $x = -s$, when $b_z = \pi$. The self-imaging period for the shifted Gaussian beam doubles to $2z_p$ because b_z equals 2π only at that distance.

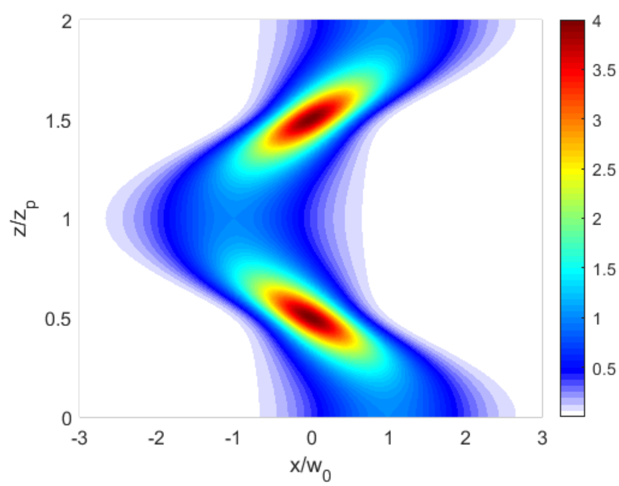

Fig 4. Evolution of an off-axis Gaussian beam (centered at $x = w_0$) inside a GRIN fiber over one self-imaging period for $C = 0.5$. Cross-section along the $y = 0$ plane is shown with a color-coded intensity distribution.

How does this doubling of the self-imaging period affect the nonlinear phenomena inside GRIN fibers? We can answer this question by using $F(\mathbf{r})$ from Eq (32) in the definition of $\bar{\gamma}(z)$ in Eq (26). The answer depends on how much the beam center is shifted initially compared to the fiber's core size. If the shift s is a small fraction of the core radius a, the effective nonlinear parameter $\bar{\gamma}(z)$ can still be approximated as $\gamma = f(z)$ with $f(z)$ given by Eq (28). Since the effective NLS Eq (27) does not change for such small shifts, they do not have a significant effect on the nonlinear properties of a GRIN fiber. In contrast, when the shift s becomes comparable to $a/2$,we cannot approximate $\bar{\gamma}(z)$ with $\gamma = f(z)$ and the doubling of the self-imaging period would impact the nonlinear phenomenon considerably. As an example, the side-band frequencies given in Eq (29) are reduced by a factor of nearly $\sqrt{2}$ for $m \neq 0$, when we replace z_p with $2z_p$.

As a second example,we consider a beam whose intensity is constant within a circle of radius r_0. For simplicity, we assume that the center of circle coincides the corecenter. In this on-axis excitation case, the beam maintains its cylindrical symmetry as its propagates down the fiber. Writing Eq (10) in the cylindrical coordinates (ρ, ϕ, z) and using $E(\rho', \phi', 0) = A_0$ for $\rho \leq r_0$ and zero for $\rho > r_0$, we obtain

$$E(\rho, \phi, ,z) = \int_0^{r_0}\int_0^{2\pi} A_0 K(\rho, \rho'; \phi, \phi')\rho' d\rho' d\phi'. \tag{33}$$

where the kernel in Eq (14) takes the form

$$K(\rho, \rho'; \phi, \phi') = \frac{\beta}{2\pi i}\left(\frac{be^{i\beta z}}{\sin(bz)}\right) \exp\left[\frac{i}{2}\beta b\cot(bz)(\rho^2 + \rho'^2) - \frac{i\beta b\rho\rho'}{\sin(bz)}\cos(\phi - \phi')\right] \tag{34}$$

The integration over ϕ' can be carried out using the known result

$$\int_0^{2\pi} \exp[-ip\cos(\phi - \phi')d\phi' = 2\pi J_0(p). \tag{35}$$

As this result does not depend on ϕ , initial radial symmetry of the input beam is maintained during its propagation inside the GRIN fiber. In the modal picture, only the radially symmetric modes are excited by such an input beam. Using Eq (35), the beam profile at a distance z is obtained using

$$E(\rho, z) = \frac{A_0\beta b e^{i\beta z}}{i\sin(bz)}\int_0^{r_0} J_0\left(\frac{\beta b\rho\rho'}{\sin(bz)}\right)\exp\left[\frac{i}{2}\beta b\cot(bz)(\rho^2 + \rho'^2)\right]\rho' d\rho'. \tag{36}$$

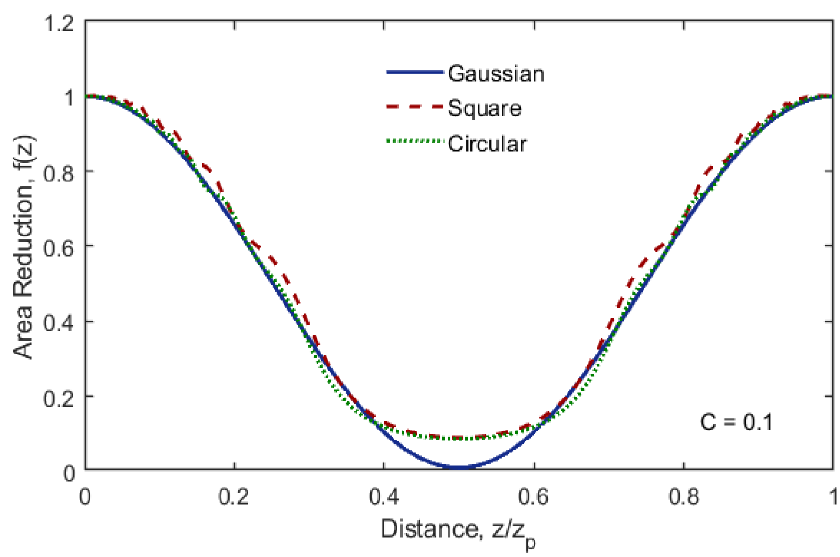

Fig 5. Variation of area reduction factor $f(z)$ over one self-imaging period for three beam shapes.

This integral must be evaluated numerically. The results show that, similar to a Gaussian beam, a circular beam also evolves periodically with a period z_p. During each period, it undergoes a compression phase and acquires a minimum spot size at a distance $z_p/2$.

We can use the preceding results to calculate the effective beam area as defined in Eq (26) and to introduce the function $f(z)$ appearing in Eq (27). Figure 5 compares $f(z)$ function for three different beam shapes for a specific value of $C = 0.1$. In the case of a Gaussian beam, we used the analytic result given in Eq (28). The curves for the circular and square apertures were calculated numerically.The circular aperture had an area of πr_0^2, whereas the area of square aperture was $4r_0^2$. Two features are note worthy. First, the minimum value of $f(z)$ occurring at the same distance $z_p/2$ is much smaller for a Gaussian beam (by a factor of about 10 for $C = 0.1$). Second, $f(z)$ exhibits oscillations for the circular and square beams that do not occur for a Gaussian beam. Both of these features are related to beam's diffraction inside a GRIN fiber, and they affect considerably the nonlinear effects inside such fibers. Our results show that the shape of input beam affects the nonlinear phenomena such as modulation instability, supercontinuum generation, and Raman-induced spectral shift of ultra short pulses [34].

6 Concluding Remarks

In this paper, which is written to celebrate the 80th birthday of Prof. Ajoy Ghatak, I have discussed how a paper that I coauthored with him in 1974 is still relevant to those studying the nonlinear effects inside GRIN fibers. We found in the 1974 paper that, even though an input beam incident on a GRIN fiber may excite hundreds of modes, the optical field at any point inside the fiber can be written, without any reference to the fiber modes, as a two-dimensional integral over the input field using a propagation kernel that is similar to that found in diffraction theory. This kernel has a specific property that reproduces the input field precisely in a periodic fashion along the length of a GRIN fiber (self-imaging).The physical origin of self-imaging lies in a ladder-like structure of the modal propagation constants with equal spacing between any two neighboring modes of the fiber.

It has been found in recent years that the periodic self-imaging also affects the nonlinear propagation of optical pulses inside multimode GRIN fibers. In this paper I first applied the general theory of self-imaging to the propagation of a CW Gaussian beam and discussed how self-imaging is modified by self-focusing produced by the Kerr nonlinearity. The case of a pulsed Gaussian beam was studied by following the approach of Ref.[13]. It resulted in a modified NLS equation that includes the effects of periodic spatial beam-width oscillations through a periodically varying effective beam area. I also showed that the formalism developed in 1974 can be used to study the impact of beam shape on the nonlinear effects inside GRIN fibers. In particular, I considered the circular and square apertures of uniform intensity.

Acknowledgments

I wish to thank Prof Ghatak for his teaching, mentoring, and friendship over the past 50 years. It is a pleasure for me that our joint work, published more than 45 years ago, is still making an impact.

References

1. Agrawal G P, Ghatak A K, Mehta C L, Propagation of a partially coherent beam through Selfoc fibers, *Opt Commun*, 12(1974)333-337.
2. Jacomme L, Modal dispersion in multimode graded-index fibers, *Appl Opt*, 14(1975)2578-2584.
3. Agrawal G P, Imaging characteristics of square law media,Nouvelle Revue d'Optique, 7(1976)299-303.
4. Olshansky R, Propagation in glass optical waveguides, *Rev Mod Phys*, 51(1979)341-367.
5. Iga K, Theory for gradient-index imaging, *Appl Opt*, 19(1980)1039-1043.
6. Richardson D J, Space-division multiplexing in optical fibres, *Nat Photon*, 7(2013)354-362.

7. Essiambre R.-J, Ryf R, Fontaine N K, Randel S, Space-division multiplexing in multimode and multicore fibers for high-capacity optical communication, *IEEE Photon J*, 5(2013)0701307; doi:10.1109/JPHOT.2013.2253091
8. Li G, Bai N, Zhao N, Xia C, Space-division multiplexing: the next frontier in optical communication, *Adv Opt Photon*, 6(2014)413-487.
9. Mafi A, Pulse propagation in a short nonlinear graded-index multi-mode optical fiber, *J Light Wave Technol*, 30(2012)2803-2811.
10. Renninger W H, Wise F W, Optical solitons in graded-index multimode fibres, *Nat Commun*, 4(2013)1719; doi: 10.1038/ncomms2739.
11. Krupa K, Tonello A, Barthélémy A, Couderc V, Shalaby B M, Bendahmane A, Millot G, Wabnitz S, Observation of geometric parametric instability induced by the periodic spatial self-imaging of multimode waves, *Phys Rev Lett*, 116(2016)183901; doi.org/10.1103/PhysRevLett.116.183901
12. Krupa K, Couderc V, Tonello A, Picozzi A, Barthélémy A, Millot G, Wabnitz S, Spatiotemporal nonlinear dynamics in multimode fibers, in Nonlinear Guided Wave Optics, (Ed) Wabnitz S, (IOP Science), Chap 14, 2014.
13. Conforti M, Arabi C M, Mussot A, Kudlinski A, Fast and accurate modeling of nonlinear pulse propagation in graded-index multimode fibers, *Opt Lett*, 42(2017)4004-4007.
14. Wright L G, Ziegler Z M, Lushnikov P M, Zhu Z, Eftekhar M A, Christodoulides D N, Wise F W, Multimode nonlinear fiber optics: massively parallel numerical solver, tutorial, and outlook, *IEEE Journal of Selected Topics in Quantum Electronics*, 24, 5100516(2018); doi: 10.1109/JSTQE.2017.2779749
15. Ahsan A S, Agrawal G P, Graded-index solitons in multimode fibers, *Opt Lett*, 43(2018)3345-3348.
16. Agrawal G P, Self-imaging in multimode graded-index fibers and its impact on the nonlinear phenomena, *Opt Fiber Technol*, 50 (2019)309-316.
17. Ghatak A, Thyagarajan K, An Introduction to Fiber Optics, (Cambridge University Press), 1999.
18. Agrawal G P, Nonlinear Fiber Optics, 6th edn, (Academic Press), 2020.
19. Ponomarenko Sergey A, Self-imaging of partially coherent light in graded-index media, *Opt Lett*, 40(2015)566-568.
20. Boyd R W, Nonlinear Optics,3 rd edn, (Academic Press), 2008.
21. Karlsson M, Anderson D, Desaix M, Dynamics of self-focusing and self-phase modulation in a parabolic index optical fiber, *Opt Lett*, 17(1992)22-24.
22. Poletti F, Horak P, Description of ultrashort pulse propagation in multimode optical fibers, *J Opt Soc Am B*, 25(2008)1645-1654.
23. Longhi S, Modulation in stability and space-time dynamics in nonlinear parabolic-index optical fiber, *Opt Lett*, 28(2003)2363-2365.
24. Lopez-Aviles H E, Wu F O, Eznaveh Z S, Eftekhar M A, Wise F, Correa R A, Christodoulides D N, Asystematic analysis of parametric instabilities in nonlinear parabolic multimode fibers, *APLPhoton*, 4, 022803(2019); doi:10.1063/1.5044659
25. Matera F, Mecozzi A, Romagnoli M, Settembre M, Side band instability induced by periodic power variation in long-distance fiber links, *Opt Lett*, 18(1993)1499-1501.
26. Hasegawa A, Self-confinemen to multimode optical pulse in a glass fiber, *Opt Lett*, 5(1980)416-417.
27. Crosignani B, Porto P D, Soliton propagation in multimode optical fibers, *Opt Lett*, 6(1981)329-330.
28. S.-S. Yu, Chien C.-H, Lai Y, Wang J, Spatio-temporal solitary pulses in graded-index materials with Kerr nonlinearity, *Opt Commun*, 119(1995)167-170.
29. Raghavan S, Agrawal G P, Spatiotemporal solitons in inhomogeneous nonlinear media, *Opt Commun*, 180(2000)377-382.
30. Kivshar Y S, Agrawal G P, Optical Solitons: From Fibers to Photonic Crystals, (Academic Press), Chap 7, 2003,
31. Lin Q, Agrawal G P, Raman response function for silica fibers, *Opt Lett*, 31(2006)3086-3088.
32. Wright L G, Wabnitz S, Christodoulides D N, Wise F W, Ultrabroadband dispersive radiation by spatiotemporal oscillation of multimode waves, *Phys Rev Lett*, 115(2015)223902; doi.org/10.1103/PhysRevLett.115.223902

33. Ahsan A S, Agrawal G P, Spatio-temporal enhancement of Raman-induced frequency shifts in graded-index multimode fibers, *Opt Lett*, 44(2019)2637-2640.
34. Ahsan A S, Agrawal G P, Effect of beam shape on the nonlinear effects inside a graded-index fiber, *J Opt Soc Am B*, (submitted).

[*Received*: 6.8.2019]

Biography

Govind P. Agrawal

Govind P. Agrawal received the B.Sc. degree from the University of Lucknow in 1969 and the M.Sc. and Ph.D. degrees from the Indian Institute of Technology, New Delhi in 1971 and 1974, respectively.

After holding positions at Ecole Polytechnic, France, City University of New York, and Bell Laboratories, NJ, Dr. Agrawal joined in 1989 the faculty of the Institute of Optics at the University of Rochester, where he holds the positions of Professor of Optics, Professor of Physics, and LLE Senior Scientist. His research interests span from optical communications and semiconductor lasers to nonlinear fiber optics and silicon photonics. He is an author or coauthor of more than 450 research papers and eight books including Fiber-Optic Communication Systems (4th ed., Wiley 2010) and Nonlinear Fiber Optics (6th ed., Academic Press 2019). These two books are used worldwide for graduate teaching and have helped in training a whole generation of scientists.

Dr Agrawal is a Fellow of the Optical Society of America (OSA) and a Life Fellow of the Institute of Electrical and Electronics Engineers (IEEE). He is also a Life Fellow of the Optical Society of India. From 2008 to 2010 Dr. Agrawal chaired the Publication Council of OSA and was a member of its Board of Directors. From 2014 to 2019 he served as the Editor-in-Chief of the OSA Journal Advances in Optics and Photonics. His alma mater, Indian Institute of Technology, gave him in 2000 its Distinguished Alumni Award. In 2012, IEEE Photonics Society honored him with its Quantum Electronics Award. He received the 2013 William H. Riker University Award for Excellence in Graduate Teaching. In 2015, he was awarded the Esther Hoffman Beller Medal of the Optical Society. Agrawal was the recipient of two major awards in 2019: Max Born Award of the Optical Society and Quantum Electronics Prize of the European Physics Society.